PCCP

Cite this: *Phys. Chem. Chem. Phys.*, 2012, **14**, 9774–9784

www.rsc.org/pccp

PAPER

Tailoring carrier injection efficiency to improve the carrier balance of solid-state light-emitting electrochemical cells

Chih-Teng Liao,[a] Hsiao-Fan Chen,[b] Hai-Ching Su*[a] and Ken-Tsung Wong*[b]

Received 8th March 2012, Accepted 9th May 2012
DOI: 10.1039/c2cp40739f

We study the influence of the carrier injection efficiency on the performance of light-emitting electrochemical cells (LECs) based on a hole-preferred transporting cationic transition metal complex (CTMC) $[Ir(dfppz)_2(dtb\text{-}bpy)]^+(PF_6^-)$ (complex **1**) and an electron-preferred transporting CTMC $[Ir(ppy)_2(dasb)]^+(PF_6^-)$ (complex **2**) (where dfppz is 1-(2,4-difluorophenyl) pyrazole, dtb-bpy is 4,4′-di(*tert*-butyl)-2,2′-bipyridine, ppy is 2-phenylpyridine and dasb is 4,5-diaza-9,9′-spirobifluorene). Experimental results show that even with electrochemically doped layers, the ohmic contacts for carrier injection could be formed only when the carrier injection barriers were relatively low. Thus, adding carrier injection layers in LECs with relatively high carrier injection barriers would affect carrier balance and thus would result in altered device efficiency. Comparison of the device characteristics of LECs based on complex **1** and **2** in various device structures suggests that the carrier injection efficiency of CTMC-based LECs should be modified according to the carrier transporting characteristics of CTMCs to optimize device efficiency. Hole-preferred transporting CTMCs should be combined with an LEC structure with a relatively high electron injection efficiency, while a relatively high hole injection efficiency would be required for LECs based on electron-preferred transporting CTMCs. Since the tailored carrier injection efficiency compensates for the unbalanced carrier transporting properties of the emissive layer, the carrier recombination zone would be located near the center of the emissive layer and exciton quenching near the electrodes would be significantly mitigated, rendering an improved device efficiency approaching the upper limit expected from the photoluminescence quantum yield of the emissive layer and the optical outcoupling efficiency from a typical layered light-emitting device structure.

Introduction

Solid-state light-emitting electrochemical cells (LECs) possess several advantages over conventional organic light emitting diodes (OLEDs). In LECs, electrochemically doped regions induced by spatially separated ions under a bias significantly reduce the barrier of carrier injection, giving balanced carrier injection, low operating voltages, and consequently high power efficiencies.[1,2] As such, LECs generally require only a single emissive layer, which can be easily processed from solutions and can conveniently use air-stable electrodes, while OLEDs typically require more sophisticated multilayer structures and low-work-function cathodes.[3,4] Compared with conventional polymer LECs that are usually composed of an emissive conjugated polymer, a salt and an ion-conducting polymer,[1,2] LECs based on cationic transition metal complexes (CTMCs) show several further advantages and have attracted much attention in recent years.[5–56] In such devices, no ion-conducting material is needed since these CTMCs are intrinsically ionic. Furthermore, higher electroluminescent (EL) efficiencies are expected due to the phosphorescent nature of CTMCs. Another benefit of employing CTMCs as the emissive materials is that they can be processed by spin coating rather than by thermal evaporation, which is commonly used in fabricating conventional multilayered OLEDs. Thus, blue-green emitting complexes, which often contain fluorinated ligands, are not subject to high temperatures and subsequent de-fluorination at elevated temperatures.[57,58]

Device efficiencies of LECs based on CTMCs are determined by the photoluminescence quantum yields (PLQYs) of the CTMCs, the spin dependent exciton harvesting ratio, the carrier balance of the devices and the optical outcoupling efficiency from a typical layered light-emitting device structure. Since CTMCs are phosphorescent materials, both singlet and triplet excitons can be harvested *via* efficient spin-orbital

[a] *Institute of Lighting and Energy Photonics, National Chiao Tung University, Tainan 71150, Taiwan. E-mail: haichingsu@mail.nctu.edu.tw; Fax: +886-6-3032535; Tel: +886-6-3032121-57792*
[b] *Department of Chemistry, National Taiwan University, Taipei 10617, Taiwan. E-mail: kenwong@ntu.edu.tw; Fax: +886-2-33661667; Tel: +886-2-33661665*

coupling mediated by the heavy-metal center. The carrier balance of the devices depends on the carrier injection efficiency and carrier transport mobilities of CTMCs. The optical outcoupling efficiency is *ca.* 20% for common layered bottom emitting device structures.[34] With perfect carrier balance in devices, the carrier injection efficiency from the electrodes and the carrier transport mobilities of CTMCs compensate for each other, *i.e.*, LECs based on CTMCs with higher electron and hole mobilities combined with device structures with higher hole and electron injection efficiencies, respectively. Hence, the carrier recombination zone would be located near the center of the emissive layer, eliminating exciton quenching near the electrodes.[59,60] Under such conditions, only the PLQYs of CTMCs and the optical outcoupling efficiency would limit LEC device efficiencies. However, many reported device efficiencies of LECs based on CTMCs[29,31,33,35,39,40,43,45,50,54] are lower than the upper limits expected from the PLQYs of their emissive layers and optical outcoupling efficiencies of $\sim$20%,[34] implying the commonly observed imperfect carrier balance in CTMC-based LECs. Furthermore, altered device efficiencies of LECs based on CTMCs when cathodes with different work functions are used have been reported.[13,16,23,36] This suggests that electrochemical doping would lower the carrier injection barrier, but would not always lead to an ohmic contact for carrier injection. Therefore, tailoring the carrier injection efficiency would affect the carrier balance and would be useful in optimizing the device efficiencies of LECs. The effects of the electrode work functions on the device characteristics of planar-type polymer LECs, which use interdigitated electrodes with spacings up to 1 mm have been systematically studied.[61] These spacings are much larger than the interelectrode distance in sandwich-type devices (typically $<$200 nm). The carrier balance would be significantly different between planar- and sandwich-type LECs due to the large discrepancy in the thickness of the active layer, which alters the intensity of the electric field and consequently affects the field-dependent electron and hole mobilities. To clarify the effects of carrier injection on the carrier balance and the consequent device efficiency of sandwich-type LECs, which are more suitable for practical applications, systematic studies of the device characteristics influenced by carrier injection barriers are highly desired. To the best of our knowledge, related reports about this issue have been scarce up to now.

In this work, we systematically study the influence of the carrier injection efficiency on the performance of LECs based on two CTMCs with oppositely preferred carrier transporting characteristics, *i.e.*, one prefers hole transport and the other prefers electron transport. The carrier injection barrier is adjusted by employing a proper hole injection layer (HIL) and/or electron injection layer (EIL). Experimental results show that an ohmic contact for the hole injection of LECs based on CTMCs would be formed by the p-type doped layer when the hole injection barrier is not high, *e.g.*, $<$0.5 eV. However, for a higher hole injection barrier, *e.g.*, $>$0.8 eV, some hole injection barrier would still exist, even with the p-type doped layer, and thus an additional HIL enhances the hole injection efficiency. Similarly, for a higher electron injection barrier, *e.g.*, $>$1.2 eV, the electron injection efficiency would be enhanced by adding an EIL since some electron injection barrier would still be present even with the n-type doped layer. Therefore, the carrier balance can be tailored by adding proper carrier injection layers for CTMC-based LECs with relatively high carrier injection barriers. To optimize the device efficiency, the carrier injection efficiency of CTMC-based LECs should be modified according to the carrier transporting characteristics of CTMCs. Hole-preferred transporting CTMCs should be combined with an LEC structure with a higher electron injection efficiency, while a higher hole injection efficiency would be required for LECs based on electron-preferred transporting CTMCs. As such, the carrier recombination zone would be located near the center of the emissive layer and exciton quenching near the electrodes would be significantly mitigated, rendering an improved device efficiency approaching the upper limit expected from the PLQY of the emissive layer and the optical outcoupling efficiency.

Experimental

Materials

The molecular structures of the two CTMCs used in this study are shown in Fig. 1. The blue-emitting CTMC $[Ir(dfppz)_2(dtb\text{-}bpy)]^+(PF_6^-)$ (**1**) (where dfppz is 1-(2,4-difluorophenyl) pyrazole and dtb-bpy is [4,4′-di(*tert*-butyl)-2,2′-bipyridine]) reported previously by Tamayo *et al.*,[19] was used as the emissive material with hole-preferred transporting characteristics.[54] The ppz-based complex $Ir(ppz)_3$ (where ppz is 1-phenylpyrazole) has been reported to be a hole transporting/electron blocking material.[62] In addition, a similar cationic complex $[Ir(dfppy)_2(bpy)]^+(PF_6^-)$ (where dfppy is 2-(2,4-difluorophenyl)pyridine and bpy is 2,2′-bipyridine) was shown to exhibit a higher hole mobility than electron mobility.[63] The device efficiencies of the LECs based on complex **1** have been shown to be significantly enhanced by doping with a low-gap hole trapping guest.[54] Since the carrier balance is improved by lowering the hole mobility of the emissive layer, complex **1** could be further proved to exhibit hole-preferred transporting characteristics.[54] On the other hand, the orange-emitting CTMC $[Ir(ppy)_2(dasb)]^+(PF_6^-)$ (**2**) (where ppy is 2-phenylpyridine and dasb is 4,5-diaza-9,9′-spirobifluorene)[26] was used as the emissive material with electron-preferred transporting characteristics. 4,5-Diaza-9,9′-spirobifluorene (dasb) is a ligand with good electron affinity, which has been used to improve the electron injection and transport properties of OLEDs for blue emitters.[64]

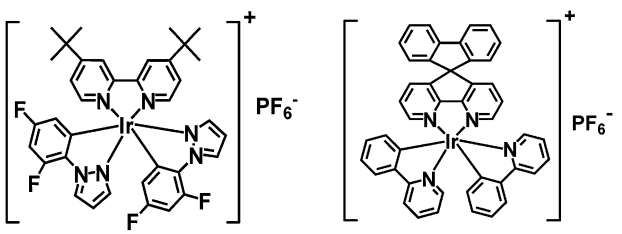

1 **2**

Fig. 1 Molecular structures of $[Ir(dfppz)_2(dtb\text{-}bpy)]^+(PF_6^-)$ (**1**) and $[Ir(ppy)_2(dasb)]^+(PF_6^-)$ (**2**).

A europium complex incorporating the dasb ligand has also been shown to exhibit a good electron-transporting ability.[65] With a device structure preferring hole injection, the LECs based on complex **2** showed high external quantum efficiencies (EQEs) up to *ca.* 9.2%, which are approaching the upper limit (*ca.* 10%) expected from the PLQY of the emissive layer (0.49) and an optical outcoupling efficiency of ~20% from a typical layered light-emitting device structure. Such a high device efficiency suggests a superior carrier balance and thus implies the electron-preferred transporting characteristics of complex **2** for compensating unbalanced carrier injection. Complex **1** and **2** were synthesized according to the procedures reported in the literature.[19,26] Thin films of the hole transporting material *N*,*N*′-diphenyl-*N*,*N*′-bis(3-methylphenyl)-1,1′-biphenyl-4,4′-diamine (TPD) were used as HILs to facilitate hole injection. For comparison, the hole transporting material *N*,*N*′-dicarbazolyl-3,5-benzene (mCP) with a high ionization potential was used to impede hole injection. Thin films of the low-work-function metal Ca were used as EILs to facilitate electron injection. The high-work-function metal Au was used to impede electron injection for comparison. To reduce the turn-on times of the LEC devices, the ionic liquid [$BMIM^+(PF_6)^-$] (where BMIM is 1-butyl-3-methylimidazolium) was added to the emissive layer to enhance the ionic conductivity of the thin films.[17] TPD (Lum Tech) and [$BMIM^+(PF_6)^-$] (Alfa Aesar) were used as received.

LEC device fabrication and characterization

Indium tin oxide (ITO)-coated glass substrates were cleaned and treated with UV/ozone prior to use. A poly(3,4-ethylenedioxythiophene):poly(styrene sulfonate) (PEDOT:PSS) (~40 nm) layer was spin-coated at 4000 rpm onto the ITO substrate in air and baked at 150 °C for 30 min. For devices without an HIL (**Device 1-S**, **1-E**, **2-S**, **2-E** and **2-IE**), the emissive layer was deposited directly on the PEDOT:PSS layer. For LEC devices with an HIL (**Device 1-H**, **1-HE**, **2-H**, **2-HE**, **2-IH** and **2-IHE**), TPD or mCP (~20 nm) was spin-coated at 5000 rpm from the chlorobenzene solutions on the PEDOT:PSS layer under ambient conditions and baked at 60 °C for 6 h. After the spin coating of the PEDOT:PSS, PEDOT:PSS/TPD or PEDOT:PSS/mCP layer, the emissive layer of complex **1** (~200 nm, for **Device 1-S**, **1-H**, **1-E** and **1-HE**) or complex **2** (~200 nm, for **2-S**, **2-H**, **2-E**, **2-HE**, **2-IH**, **2-IE** and **2-IHE**) was then spin-coated at 3000 rpm from the acetonitrile solutions under ambient conditions. The ionic liquid [$BMIM^+(PF_6)^-$] (20 wt%) was added to the emissive layer to enhance the ionic conductivity of the thin films and thus to reduce the turn-on time of the LEC device.[17] After the spin coating of all the organic layers, the thin films were baked at 70 °C for 10 h in a nitrogen glove box (oxygen and moisture levels below 1 ppm), followed by thermal evaporation of a 100 nm Ag film (**Device 1-S**, **1-H**, **2-S**, **2-H** and **2-IH**), a 40 nm Ca film (EIL) capped with an 80 nm Ag film (**Device 1-E**, **1-HE**, **2-E** and **2-HE**) and a 20 nm Au film capped with an 80 nm Ag film (**Device 2-IE** and **2-IHE**) as the top contact in a vacuum chamber (~10^{-6} torr). The thicknesses of the thin films were measured by ellipsometry. The electrical and emission characteristics of the LEC devices were measured using a source-measurement unit and an Si photodiode calibrated with the Photo Research PR-650 spectroradiometer. All the device measurements were performed under a constant bias voltage (3.5 V for **Device 1-S**, **1-H**, **1-E** and **1-HE** and 2.4 V for **2-S**, **2-H**, **2-E**, **2-HE**, **2-IH**, **2-IE** and **2-IHE**) in a nitrogen glove box. The EL spectra were taken with a calibrated CCD spectrograph.

Results and discussions

General LEC device characteristics

To clarify the effects of carrier injection on the carrier balance and thus the device efficiency the LECs, the EL characteristics of LECs of various configurations for carrier injection were measured and are summarized in Table 1. The device configurations of the LECs under study and the related energy level alignments[14,50,61,66–68] are shown in Fig. 2. The standard LECs have the structure of [ITO/PEDOT:PSS (40 nm)/complex **1** (200 nm, for **Device 1-S**) or complex **2** (200 nm, for **Device 2-S**)/Ag (100 nm)]. The LECs with HILs have the structure of [ITO/PEDOT:PSS (40 nm)/TPD (20 nm)/complex **1** (200 nm, for **Device 1-H**) or complex **2** (200 nm, for **Device 2-H**)/Ag (100 nm)]. For comparison, the LECs with HILs to impede hole injection have the structure of [ITO/PEDOT:PSS (40 nm)/mCP (20 nm)/complex **2** (200 nm, for **Device 2-IH**)/Ag (100 nm)]. The LECs with EILs have the structure of [ITO/PEDOT:PSS (40 nm)/complex **1** (200 nm, for **Device 1-E**) or complex **2**

Table 1 Summary of the LEC device characteristics

Device	Bias (V)	$\lambda_{max,EL}$ (nm)	t_{max} (min)[a]	J_{max} (mA cm^{-2})[b]	L_{max} (cd m^{-2})[c]	$\eta_{ext,max}$ (%)[d]	$\eta_{p,max}$ (lm W^{-1})[e]	Lifetime (min)[f]
1-S	3.5	483	36	0.31	19.63	8.52	16.96	27
1-H	3.5	487	29	0.45	19.05	6.76	13.55	18
1-E	3.5	484	18	0.57	73.98	9.58	18.79	12
1-HE	3.5	482	14	0.65	108.94	10.50	20.64	6
2-S	2.4	586	510	0.08	16.45	9.16	26.91	—[g]
2-H	2.4	589	532	0.08	14.26	8.68	24.91	—[g]
2-E	2.4	596	102	0.26	16.25	5.37	13.70	204
2-HE	2.4	595	73	0.27	16.52	5.66	14.83	115
2-IH	2.4	588	530	0.066	7.33	4.94	14.50	—[g]
2-IE	2.4	585	544	0.064	6.67	4.68	13.74	—[g]
2-IHE	2.4	585	600	0.056	6.61	5.27	15.48	—[g]

[a] Time required to reach the maximal brightness. [b] Maximal current density achieved at a constant bias voltage. [c] Maximal brightness achieved at a constant bias voltage. [d] Maximal external quantum efficiency achieved at a constant bias voltage. [e] Maximal power efficiency achieved at a constant bias voltage. [f] Time for the brightness of the device to decay from the maximum to half of the maximum under a constant bias voltage. [g] Lifetime can not be determined since the brightness has not decreased to half of the maximum value during measurement.

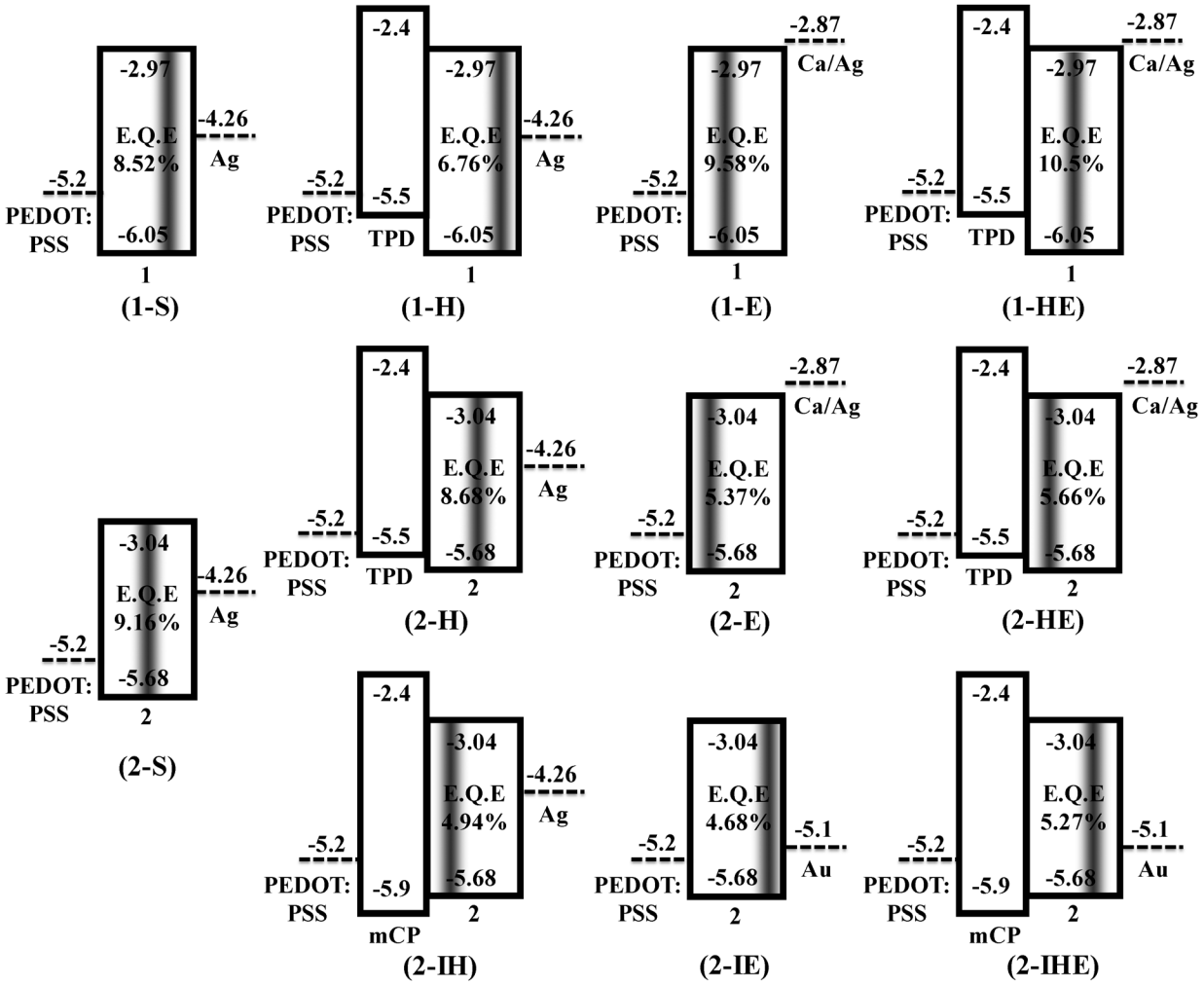

Fig. 2 Device configurations, energy level alignments and schematic diagrams of the position of carrier recombination zone for the LECs under study. The electrochemically doped regions near the electrodes are omitted for clarity.

(200 nm, for **Device 2-E**)/Ca (40 nm)/Ag (80 nm)]. For comparison, the LECs with EILs to impede electron injection have the structure of [ITO/PEDOT:PSS (40 nm)/complex **2** (200 nm, for **Device 2-IE**)/Au (20 nm)/Ag (80 nm)]. The LECs with both HILs and EILs have the structure of [ITO/PEDOT:PSS (40 nm)/TPD (20 nm)/complex **1** (200 nm, for **Device 1-HE**) or complex **2** (200 nm, for **Device 2-HE**)/Ca (40 nm)/Ag (80 nm)]. For comparison, the LECs with both HILs and EILs to impede both hole and electron injection have the structure of [ITO/PEDOT:PSS (40 nm)/mCP (20 nm)/complex **2** (200 nm, for **Device 2-IHE**)/Au (20 nm)/Ag (80 nm)]. The EL spectra of **Devices 1-S, 1-H, 1-E** and **1-HE** at 3.5 V and **2-S**, **2-H**, **2-E**, **2-HE**, **2-IH**, **2-IE** and **2-IHE** at 2.4 V are shown in Fig. 3. The LECs based on complex **1** (**Devices 1-S**, **1-H**, **1-E** and **1-HE**) exhibited similar EL spectra, dominated by the emission of complex **1**. For the LECs based on complex **2** (**2-S**, **2-H**, **2-E**, **2-HE**, **2-IH**, **2-IE** and **2-IHE**), the predominant EL emission resulted from complex **2**. These results reveal that the carrier recombination zone is still mainly located in the CTMC layer, even when carrier injection layers are added. Therefore, discrepancies in device characteristics when different device configurations are employed can be reasonably attributed to the altered carrier balance induced by different carrier injection efficiencies.

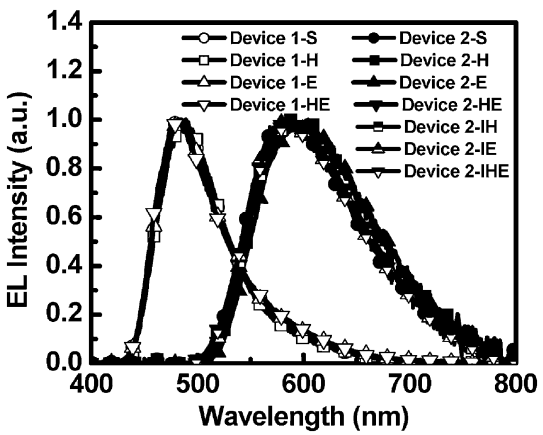

Fig. 3 EL spectra of **Devices 1-S**, **1-H**, **1-E** and **1-HE** at 3.5 V and **Devices 2-S**, **2-H**, **2-E**, **2-HE**, **2-IH**, **2-IE** and **2-IHE** at 2.4 V.

The time-dependent current density, brightness and EQE of **Devices 1-S**, **1-H**, **1-E** and **1-HE** at 3.5 V, **Devices 2-S**, **2-H**, **2-E**

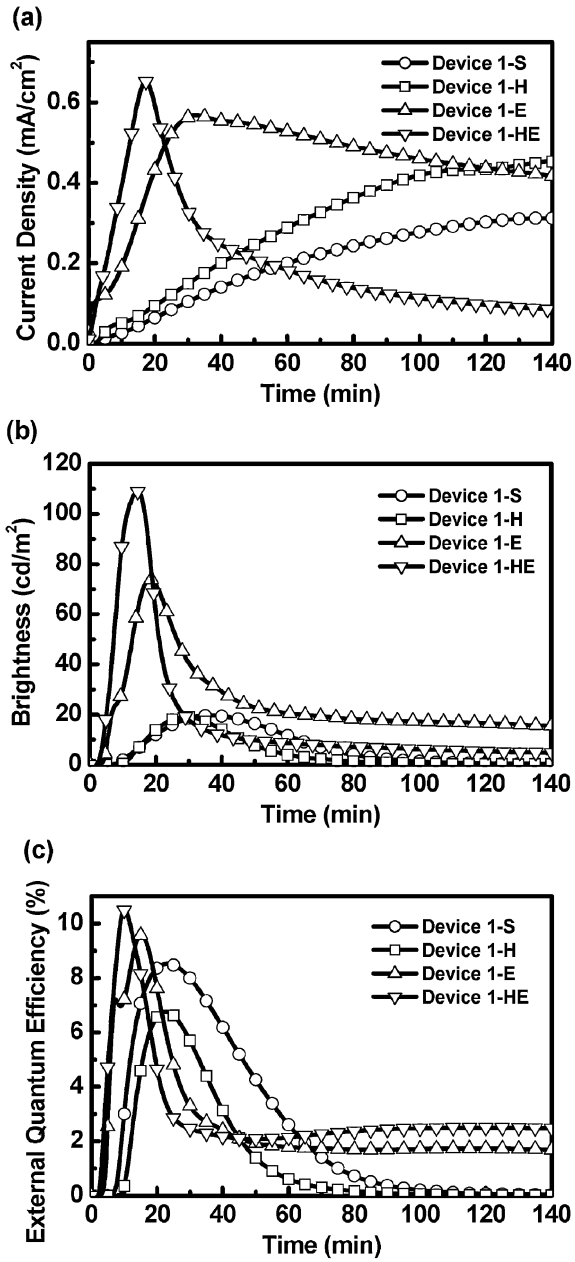

Fig. 4 (a) Current density, (b) brightness and (c) external quantum efficiency as a function of time for **Devices 1-S**, **1-H**, **1-E** and **1-HE** at 3.5 V.

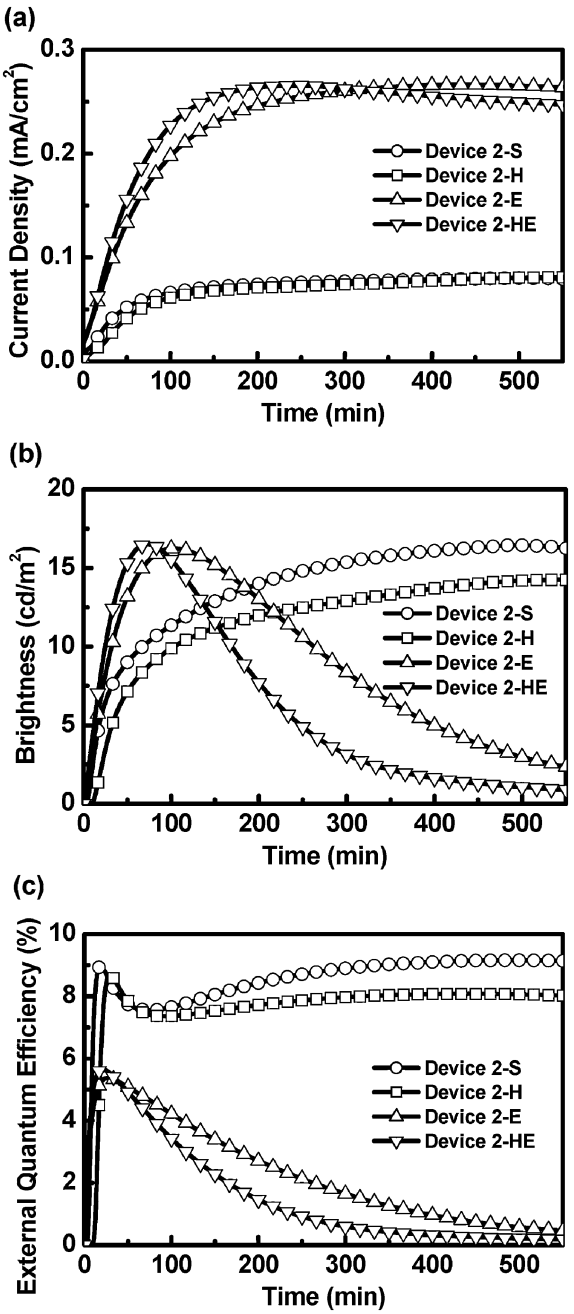

Fig. 5 (a) Current density, (b) brightness and (c) external quantum efficiency as a function of time for **Devices 2-S**, **2-H**, **2-E** and **2-HE** at 2.4 V.

and **2-HE** at 2.4 V and **Devices 2-IH**, **2-IE** and **2-IHE** at 2.4 V are shown in Figs. 4(a)–(c), 5(a)–(c) and 6(a)–(c), respectively. All the LECs exhibited similar trends in the time-dependent EL characteristics under constant-bias operation. After the bias was applied, the device current, brightness and EQE increased due to the enhanced carrier injection induced by gradually formed p- and n-type doped layers near the electrodes.[52] The brightness and EQE first increased with the device current and reached the maximum values. Then they dropped over time with a rate depending on the bias voltage (or current). The drop in brightness and device efficiency after reaching the peak value, as commonly seen in solid-state CTMC-based LECs,[5–56] may be associated with several factors. When the device current is still increasing, the p- and n-type doped layers keep extending and the carrier injection efficiency is continuously enhanced. Therefore, the carrier recombination zone may keep moving closer to one electrode due to the discrepancy in the electron and hole mobilities, which would induce exciton quenching and reduced brightness and device efficiency.[59,60] The decrease in brightness and efficiency under a relatively steady device current may be rationally attributed to the degradation of the emissive material during the LEC operation.[10] Though all the LECs exhibited similar trends in their time-dependent EL characteristics, distinctive carrier balance and thus device efficiency were observed in LECs with different carrier-injection structures.

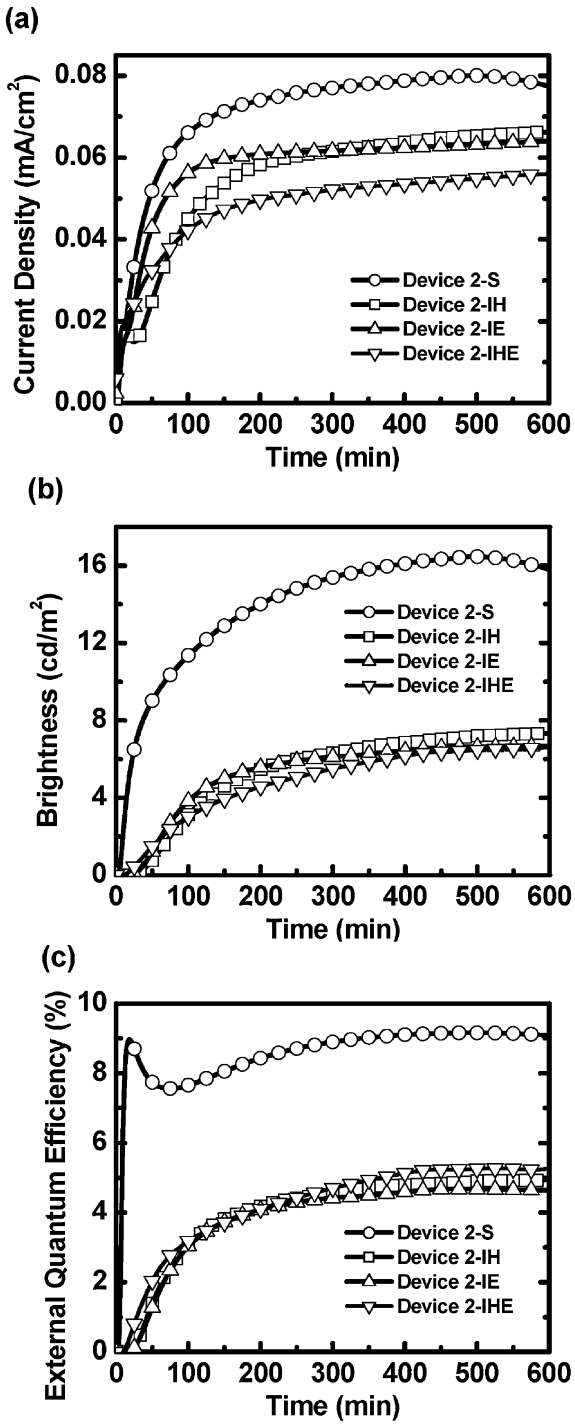

Fig. 6 (a) Current density, (b) brightness and (c) external quantum efficiency as a function of time for **Devices 2-S**, **2-IH**, **2-IE** and **2-IHE** at 2.4 V.

The effects of the improved carrier injection on the device characteristics of the LECs based on complex **1** and **2** are discussed in the following subsections.

Effects of improved hole injection on the device characteristics of LECs

Standard LECs based on complex **1** and **2** have the structure of ITO/PEDOT:PSS/emissive layer/Ag, which has been commonly used in previous reports.[50,53,54,56] It should be noted that **Device 2-S** exhibited a slower device response (the brightness is still increasing after ~10 h operation), lower brightness and higher device efficiency as compared to previously reported LECs based on the same complex.[26] These results are attributed to the different device thicknesses and bias voltages used in the two works. In ref. 26, the device thickness is 100 nm and the bias voltages are 2.6 and 2.5 V, while in this work the thickness is 200 nm and the bias voltage is 2.4 V. The increased thickness and lower bias reduce the electric field inside the emissive layer and thus lengthen the time required for mobile ions to accumulate near the electrodes, causing a slower device response. Since the brightness of the LECs in this work has not yet shown a significant decrease after 10 h operation (Fig. 5(b)), extrapolation, which has been used in ref. 26 to derive the device lifetimes, can not be used to estimate the lifetimes of the LECs in this work. The reduced electric field also leads to a lower current density, which results in a reduced brightness. However, the thicker emissive layer is beneficial in preventing exciton quenching near the electrodes. Thus, the device efficiency of **Device 2-S** is higher than that of the LECs based on the same complex.[26] The hole injection efficiency of the standard LECs based on complex **1** and **2** was tailored by adding an HIL (TPD) between the PEDOT:PSS and the emissive layer (**Device 1-H** *vs.* **1-S** and **Device 2-H** *vs.* **2-S**, Fig. 2). For the LECs based on complex **1**, the device current was significantly enhanced by inserting an HIL (Fig. 4(a)). Although there is a slight voltage drop across a thin neutral HIL (20 nm), the reduced hole injection barrier still plays a major role in the device characteristics and thus the device current was enhanced. However, the device current of the LECs based on complex **2** remained approximately unchanged after an HIL was added (Fig. 5(a)). Furthermore, since the LECs based on complex **1** with and without an HIL exhibited a similar brightness (Fig. 4(b)), the EQE of the device with an HIL, which exhibited a much higher device current, was much lower than that of the device without an HIL (Fig. 4(c)). On the other hand, for the LECs based on complex **2**, only slight discrepancies in the brightness and consequent device efficiency were measured for devices with and without an HIL (Fig. 5(b) and (c)). These results reveal that the device characteristics of the LECs based on complex **2** are insensitive to the hole injection barrier, while the carrier balance is significantly altered by the insertion of an HIL for the LECs based on complex **1**.

For CTMCs with lower energy gaps, *e.g.*, complex **2**, the energy barrier for hole injection is moderate (0.48 eV) and thus an ohmic contact for hole injection would be formed by the p-type doped layer. The similar maximum device current and time to reach the maximum brightness for standard LECs based on complex **2** without and with an HIL (**Devices 2-S** and **2-H**, Table 1) reveal similar hole injection efficiencies and formation rates of the p-type doped layer, confirming the formation of ohmic contacts for hole injection for both devices. Thus, the additional HIL has little effect on the p-type electrochemical doping processes and consequent carrier balance, leading to almost unchanged device efficiencies (**Devices 2-S** and **2-H**, Fig. 5(c)). Both the standard LECs based on complex **2** without and with an HIL showed similarly high EQEs up to

ca. 9%, which is approaching the upper limit (9.8%) expected from the PLQY of the emissive layer (0.49) and an optical outcoupling efficiency of ~20% from a typical layered light-emitting device structure. Such high device efficiencies highlight the superior carrier balance of the standard LECs based on complex **2**. Since the energy barrier for electron injection (1.22 eV) is much larger than that for hole injection (0.48 eV) in the standard LECs based on complex **2** (**Device 2-S**, Fig. 2), complex **2** possesses electron-preferred transporting characteristics that compensate for the unbalanced hole-preferred carrier injection, resulting in a good carrier balance.

On the other hand, for CTMCs with higher energy gaps, *e.g*., complex **1**, the p-type doped layer is not capable of providing an ohmic contact with the anode when the hole injection barrier is large (0.85 eV, **Device 1-S**, Fig. 2). The higher maximum device current and shorter time to reach the maximum brightness for the standard LECs based on complex **1** with an HIL, as compared to those without an HIL (**Device 1-H** *vs*. **1-S**, Table 1), reveal a higher hole injection efficiency and faster formation of the p-type doped layer. The additional HIL significantly accelerates the p-type electrochemical doping processes since fewer accumulated anions near the anode are required to enhance hole injection for devices with a smaller hole injection barrier (**Device 1-H**). As the p-type layer is well established, the hole injection efficiency of the standard LECs with an HIL is much higher than that without an HIL, confirming that ohmic contact for hole injection can not be achieved in devices with a higher hole injection barrier (**Device 1-S**). Therefore, the addition of an HIL in the LECs based on complex **1** leads to an altered carrier balance and device efficiency (**Device 1-H** *vs*. **1-S**, Fig. 4(c)). Since complex **1** has been reported to exhibit hole-preferred transporting characteristics,[54] the carrier recombination zone in the standard LECs based on complex **1** would be located near the cathode due to the smaller hole injection barrier (**Device 1-S**, Fig. 2). Exciton quenching occurs when the carrier recombination zone approaches the electrodes and the device efficiency consequently deteriorates.[59,60] The standard LECs based on complex **1** showed EQEs of *ca*. 8.5%, which is much lower than that expected (15%) from the PLQY of the thin film of complex **1** (0.75),[54] and an optical outcoupling efficiency of ~20% from a typical layered light-emitting device structure. Such a reduced device efficiency confirms the poor carrier balance of the standard LECs based on complex **1**. With an HIL, the carrier recombination zone of the LECs based on complex **1** (**Device 1-H**, Fig. 2) is further pushed towards the cathode due to the enhanced hole injection efficiency, resulting in more severe exciton quenching and even a reduced EQE (*ca*. 6.8%, Table 1). These results suggest that an ohmic contact for the hole injection of LECs based on CTMCs can be formed only when the energy barrier for hole injection is not large. For most blue-emitting CTMCs, in which the highest occupied molecular orbital (HOMO) levels are stabilized by fluoro substitution to increase the energy gaps,[19,29,31,38,43,46,48,50,54,56] the energy barrier for hole injection is commonly large in standard LECs using, for example, ITO as the anode material. Hence, the carrier balance of standard LECs based on CTMCs with higher energy gaps can be adjusted by tailoring the hole injection efficiency with proper HILs. However, an enhanced hole injection efficiency may not necessarily lead to an improved device efficiency, *e.g*., for LECs based on CTMCs with hole-preferred transporting characteristics. For such LECs, a large hole injection barrier to reduce the number of holes compensates for the excess holes in the emissive layer, resulting in a better carrier balance.

Effects of improved electron injection on the device characteristics of LECs

The electron injection efficiency of standard LECs based on complex **1** and **2** was tailored by inserting a low-work-function EIL (Ca) at the cathode (**Device 1-E** and **Device 2-E**, Fig. 2). Both devices employing Ca cathodes showed much higher device current as compared to standard devices with Ag cathodes (Fig. 4(a) and 5(a)) due to the enhanced electron injection. However, when an EIL was incorporated, the device efficiency of the LECs base on complex **1** increased, while that of the LECs base on complex **2** decreased compared to their standard Ag-cathode counterparts (**Device 1-E** *vs*. **1-S**, Fig. 4(c) and **Device 2-E** *vs*. **2-S**, Fig. 5(c)). Therefore, the addition of EILs in standard LECs based on complex **1** and **2** alters the carrier balance of both devices. Since standard LEC devices based on both complexes, which exhibit similar lowest unoccupied molecular orbital (LUMO) levels, possess high electron injection barriers when Ag is used as the cathode (1.29 and 1.22 eV for complex **1** and **2**, respectively, Fig. 2), these results indicate that the n-type doped layer is not capable of providing an ohmic contact with the cathode when the electron injection barrier is high. The significantly higher maximum device current and much shorter time required to reach the maximum brightness for the LECs based on complexes **1** and **2** with Ca cathodes, as compared to those with Ag cathodes (**Device 1-E** *vs*. **1-S** and **Device 2-E** *vs*. **2-S**, Table 1), indicate a higher electron injection efficiency and a faster formation of the n-type doped layer. The low-work-function Ca cathode significantly accelerates the n-type electrochemical doping processes since much fewer accumulated cations near the cathode are required to enhance the electron injection for the almost eliminated electron injection barrier (**Device 1-E** and **Device 2-E**, Fig. 2). As the n-type layer is well established, the electron injection efficiency of the LECs with Ca cathodes is much higher than that with Ag cathodes, confirming that ohmic contact for electron injection can not be achieved in devices with a higher electron injection barrier (**Device 1-S** and **2-S**). Thus, the addition of an EIL leads to an altered carrier balance and device efficiency (**Device 1-E** *vs*. **1-S**, Fig. 4(c) and **Device 2-E** *vs*. **2-S**, Fig. 5(c)).

For the LECs based on complex **1**, the enhanced electron injection induced by the Ca cathode pushes the carrier recombination zone away from the cathode and consequently mitigates exciton quenching, leading to improved device efficiency compared to the devices with Ag cathodes (**Device 1-E** *vs*. **1-S**, Fig. 2). In contrast, for the LECs based on complex **2**, the enhanced electron injection induced by the Ca cathode deteriorates the carrier balance and the carrier recombination zone is shifted towards the anode, resulting in severe exciton quenching and thus a reduced device efficiency (**Device 2-E** *vs*. **2-S**, Fig. 2). The improved device efficiencies of LECs based

on CTMCs have been reported when low-work-function cathode metals are used.[13,16,36] These results also suggest that the electron injection of LECs with a higher injection barrier, *e.g.*, using inert high-work-function cathodes, is not ohmic and thus the carrier balance is altered when the electron injection efficiency is adjusted. Additionally, in this work, we demonstrate that an enhanced electron injection efficiency does not necessarily lead to an improved device efficiency. Enhancing the electron injection efficiency improves the carrier balance of the LECs based on CTMCs with hole-preferred transporting characteristics, *e.g.*, complex **1**. The increased amount of injected electrons compensates for the unbalanced hole-preferred transporting characteristics of CTMCs, leading to a better carrier balance. However, for the LECs based on CTMCs with electron-preferred transporting characteristics, *e.g.*, complex **2**, the enhanced electron injection efficiency resulted in excess electrons and thus a poorer carrier balance. For such devices, inert high-work-function cathodes, which are ineffective in electron injection, could be used instead to reduce the number of electrons in the emissive layer and thus to improve the carrier balance.

Effects of improved hole and electron injection on the device characteristics of LECs

The hole and electron injection efficiencies of the standard LECs based on complex **1** and **2** were simultaneously tailored by adopting both an HIL and an EIL (**Device 1-HE** and **Device 2-HE**, Fig. 2). For the LECs based on complex **1** with an HIL and an EIL, the device current was higher than that of the HIL-only (**Device 1-H**) and the EIL-only devices (**Device 1-E**), confirming that both hole and electron injection efficiencies are enhanced (Fig. 4(a)). For the LECs based on complex **2** with an HIL and an EIL, the device current was also higher than that of the HIL-only devices (**Device 2-H**), indicating improved electron injection (Fig. 5(a)). However, the device current of the LECs based on complex **2** with an HIL and an EIL was similar to that of the EIL-only devices (**Device 2-E**) (Fig. 5(a)). It reveals that the enhanced device current of the LECs base on complex **2** employing both an HIL and an EIL is dominated by the increased electron current and the HIL has little effect on the hole injection efficiency, which is consistent with the results comparing the standard LECs based on complex **2** with and without an HIL (**Device 2-S** *vs.* **2-H**, Fig. 5(a)). The LECs based on complex **1** with an HIL and an EIL exhibited a faster device response compared to the HIL-only (**Device 1-H**) and EIL-only devices (**Device 1-E**) since much fewer accumulated cations near the cathode and anions near the anode are required to enhance the injection efficiency of electrons and holes, respectively (Table 1). A faster device response was also observed for the LECs based on complex **2** with an HIL and an EIL when compared with the HIL-only devices (**Device 2-H**) (Table 1) for the same reason. However, it is noted that although the HIL has little effect on the hole injection efficiency, the LECs based on complex **2** with an HIL and an EIL still exhibited a faster device response than the EIL-only devices (**Device 2-E**) (Table 1). Since the electron injection barrier is rather small when Ca is used as the cathode, the n-type doped layer capable of achieving ohmic contact for electron injection is rapidly formed at the cathode and thus most of the voltage drop takes place across the thinner intrinsic emissive layer, before the p-type doped layer for efficient hole injection is well established.[52] Thus, with an HIL for reducing the hole injection barrier, a higher electric field in the thinner intrinsic emissive layer accelerated the accumulation of enough anions to form the p-type doped layer for efficient hole injection, leading to a faster device response. After reaching the steady state, the hole injection of both devices at the anode became ohmic due to the smaller hole injection barriers and thus the maximum device current of both devices were similar (**Device 2-E** and **Device 2-HE**, Fig. 5(a)). In contrast, the standard LECs based on complex **2** with and without an HIL (**Device 2-S** and **2-H**) exhibited comparable device responses (Table 1). Since both devices employing Ag cathodes possess a high electron injection barrier, the device response is mainly dominated by the slower formation of the n-type doped layer. Similar device response times of both devices were thus measured (**Device 2-S** and **2-H**, Table 1).

The LECs based on complex **1** employing both an HIL and an EIL showed better device efficiencies than the EIL-only devices (**Device 1-E**). This reveals that significantly enhanced electron injection in the EIL-only devices results in more electrons than holes in the emissive layer and the carrier recombination zone is consequently closer to the p-type doped layer. With an additional HIL, the number of injected holes increases and the carrier recombination zone moves toward the center of the emissive layer, leading to reduced exciton quenching and a higher device efficiency. Compared with the EQE of the standard LECs based on complex **1** (*ca.* 8.5%), the EQE of the LECs based on complex **1** employing both an HIL and an EIL (10.5%) was enhanced by 24% (**Device 1-HE** *vs.* **Device 1-S**, Table 1). This confirms that properly modifying the carrier injection efficiency according to the carrier transporting characteristics of the emissive materials can optimize the device efficiencies of LECs based on CTMCs. In contrast, the LECs based on complex **2** employing both an HIL and an EIL exhibited similar device efficiencies to the EIL-only devices (**Device 2-E**). Since the hole injection barrier is relatively low for the standard LECs based on complex **2**, an ohmic contact for hole injection is achieved with the p-type doped layer whether the HIL is added or not. Therefore, the carrier balance of the LECs based on complex **2** employing both an HIL and an EIL is similar to that of the EIL-only devices (**Device 2-HE** *vs.* **Device 2-E**, Fig. 2). The significantly reduced device efficiencies of both LECs (5.37 and 5.66% for **Device 2-E** and **Device 2-HE**, respectively) compared to the standard LECs based on complex **2** (*ca.* 9.2%, **Device 2-S**) indicate that over-enhancing the electron injection of LECs based on CTMCs with electron-preferred transporting characteristics is detrimental to the carrier balance. Similarly, over-enhancing the hole injection of the LECs based on CTMCs with hole-preferred transporting characteristics also leads to a poor carrier balance (**Device 1-H**, Fig. 2). To optimize device efficiency, the carrier injection efficiency should be tailored to compensate for the imbalance in the carrier transporting characteristics of CTMCs. Such a technique could optimize LECs with higher carrier injection barriers since electrochemically

doped layers are not capable of providing ohmic contacts for carrier injection. The carrier injection efficiency and consequent carrier balance could be effectively modified by employing proper carrier injection layers.

Effects of impeded hole, electron and both hole and electron injection on the device characteristics of LECs

Since LECs based on complex **2** exhibited a poor carrier balance with enhanced hole and/or electron injection, it would be interesting to study the device characteristics when the carrier injection is impeded. Impeded hole and electron injection of the LECs based on complex **2** was achieved by inserting a hole transporting layer with a high ionization potential (mCP) at the anode and employing a high-work-function metal (Au) at the cathode (**Devices 2-IH**, **2-IE** and **2-IHE**, Fig. 2). As shown in Fig. 6(a), the LECs based on complex **2** with impeded hole (**Device 2-IH**) and electron injection (**Device 2-IE**) showed lowered device currents than the standard LECs based on complex **2** (**Device 2-S**) under the same bias voltage. With impeded hole and electron injection (**Device 2-IHE**), the device current further declined. This confirms that electrochemically doped layers are not capable of providing ohmic contacts for large carrier injection barriers (>0.7 eV, Fig. 2). Compared with **Device 2-S**, the LECs based on complex **2** with impeded carrier injection also exhibited a slower device response (Fig. 6(b) and Table 1) since the time required for mobile ions to accumulate near the electrodes to facilitate carrier injection is lengthened when the carrier injection barrier is large. Furthermore, the much lower brightness of the LECs based on complex **2** with impeded carrier injection implied a significantly reduced device efficiency compared to **Device 2-S**. As shown in Fig. 6(c), LECs based on complex **2** with impeded hole or electron injection showed low EQEs $<5\%$, which is only half of that obtained in **Device 2-S**. With a large hole injection barrier, the carrier balance of **Device 2-S** deteriorates and thus the carrier recombination zone is pushed toward the anode, resulting in exciton quenching and lowered EQEs (**Device 2-IH**, Fig. 2). In contrast, a significantly increased electron injection barrier shifts the carrier recombination zone toward the cathode and consequently leads to exciton quenching and lowered EQEs (**Device 2-IE**, Fig. 2). Since the enhancement in the carrier injection barrier is more significant for electrons (**Device 2-IE**) than for holes (**Device 2-IH**) compared to **Device 2-S**, which has a superior carrier balance, the deterioration in the device efficiency is more severe in **2-IE** (Table 1). It is interesting that the simultaneous enhancement in the hole and electron injection barriers of the LECs based on complex **2** (**Device 2-IHE**) leads to a slight increase in the device efficiency compared to the devices with independently impeded hole or electron injection (**Device 2-IH** or **2-IE**) (Table 1). However, the device efficiency of **2-IHE** is still far below that of **2-S**. These results indicate that the simultaneous enhancement in the hole and electron injection barriers is beneficial in improving the deteriorated carrier balance of **Devices 2-IH** and **2-IE**. However, the improvement in the device efficiency is not significant since the carrier recombination zone is only slightly shifted away from the cathode due to the unbalanced carrier injection (**Device 2-IHE**, Fig. 2).

The results mentioned in the above sections reveal that the alteration (either increase or decrease) of the carrier injection efficiency of LECs with a superior carrier balance, *e.g.*, **Device 2-S**, which exhibited high EQEs approaching the upper limit estimated form the PLQY of the emissive layer, would deteriorate the carrier balance and reduce the device efficiency.

With a judiciously tailored carrier balance, the peak EQEs of our sky-blue and orange LECs reached 10.5 and 9.16%, respectively. These results are approaching the state-of-the-art EQEs reported previously for sky-blue (12.75%)[54] and orange LECs (10.4%).[27] Thus, proposed strategy of tailoring the carrier balance by adjusting the carrier injection efficiency is effective in improving the device efficiencies of LECs. However, compared with the high EQEs of $\sim$20% achieved in conventional sky-blue[69] and orange[70] OLEDs, in which host–guest emissive layers are generally used, the device efficiencies of neat-film LECs still have much room for improvement due to the self-quenching of excitons in the condensed neat films. To further enhance the device efficiencies of LECs, electrochemically stable high-gap ionic host materials would be required, especially for blue-green LECs, to reduce the self-quenching effect. A high energy barrier for carrier injection from the electrodes would be a general problem for high-gap hosts, in which electrochemically doped layers would not be capable of providing ohmic contacts for carrier injection. Tailoring the carrier balance by adjusting the carrier injection efficiency would also be effective in improving the device efficiencies of host–guest LECs. This could be a potential technique for host–guest LECs to achieve device efficiencies comparable to conventional OLEDs in the future.

Conclusions

In summary, we have demonstrated the influence of the carrier injection efficiency on the performance of LECs employing two CTMCs (complex **1** and **2**) with oppositely preferred carrier transporting characteristics. Even with electrochemically doped layers, an ohmic contact for carrier injection could be formed only when the carrier injection barrier is relatively low. Adding carrier injection layers in LECs with relatively high carrier injection barriers enhances the carrier injection efficiency and affects the carrier balance, consequently resulting in an altered device efficiency. Furthermore, comparison of the device characteristics of LECs based on complex **1** and **2** in various device structures indicates that the carrier injection efficiency of CTMC-based LECs should be modified according to the carrier transporting characteristics of CTMCs to optimize the device efficiency. Hole-preferred transporting CTMCs should be combined with an LEC structure with a relatively high electron injection efficiency, while a relatively high hole injection efficiency is required for LECs based on electron-preferred transporting CTMCs. With a properly tailored carrier balance, the carrier recombination zone is located near the center of the emissive layer and exciton quenching near electrodes is significantly mitigated, rendering an improved device efficiency approaching the upper limit expected from the PLQY of the emissive layer and the optical outcoupling efficiency.

Acknowledgements

The authors gratefully acknowledge the financial support from the National Science Council of Taiwan.

References

1 Q. Pei, G. Yu, C. Zhang, Y. Yang and A. J. Heeger, *Science*, 1995, **269**, 1086.
2 Q. Pei, Y. Yang, G. Yu, C. Zhang and A. J. Heeger, *J. Am. Chem. Soc.*, 1996, **118**, 3922.
3 C. W. Tang and S. A. VanSlyke, *Appl. Phys. Lett.*, 1987, **51**, 913.
4 C. W. Tang, S. A. VanSlyke and C. H. Chen, *J. Appl. Phys.*, 1989, **65**, 3610.
5 J. K. Lee, D. S. Yoo, E. S. Handy and M. F. Rubner, *Appl. Phys. Lett.*, 1996, **69**, 1686.
6 C. H. Lyons, E. D. Abbas, J. K. Lee and M. F. Rubner, *J. Am. Chem. Soc.*, 1998, **120**, 12100.
7 F. G. Gao and A. J. Bard, *J. Am. Chem. Soc.*, 2000, **122**, 7426.
8 H. Rudmann and M. F. Rubner, *J. Appl. Phys.*, 2001, **90**, 4338.
9 H. Rudmann, S. Shimada and M. F. Rubner, *J. Am. Chem. Soc.*, 2002, **124**, 4918.
10 G. Kalyuzhny, M. Buda, J. McNeill, P. Barbara and A. J. Bard, *J. Am. Chem. Soc.*, 2003, **125**, 6272.
11 J. D. Slinker, D. Bernards, P. L. Houston, H. D. Abruña, S. Bernhard and G. G. Malliaras, *Chem. Commun.*, 2003, 2392.
12 H. Rudmann, S. Shimada and M. F. Rubner, *J. Appl. Phys.*, 2003, **94**, 115.
13 J. D. Slinker, A. A. Gorodetsky, M. S. Lowry, J. Wang, S. Parker, R. Rohl, S. Bernhard and G. G. Malliaras, *J. Am. Chem. Soc.*, 2004, **126**, 2763.
14 A. A. Gorodetsky, S. Parker, J. D. Slinker, D. A. Bernards, M. H. Wong, G. G. Malliarasa, S. Flores-Torres and H. D. Abruña, *Appl. Phys. Lett.*, 2004, **84**, 807.
15 A. R. Hosseini, C. Y. Koh, J. D. Slinker, S. Flores-Torres, H. D. Abruña and G. G. Malliaras, *Chem. Mater.*, 2005, **17**, 6114.
16 J. D. Slinker, C. Y. Koh, G. G. Malliaras, M. S. Lowry and S. Bernhard, *Appl. Phys. Lett.*, 2005, **86**, 173506.
17 S. T. Parker, J. D. Slinker, M. S. Lowry, M. P. Cox, S. Bernhard and G. G. Malliaras, *Chem. Mater.*, 2005, **17**, 3187.
18 M. S. Lowry, J. I. Goldsmith, J. D. Slinker, R. Rohl, R. A. Pascal, Jr., G. G. Malliaras and S. Bernhard, *Chem. Mater.*, 2005, **17**, 5712.
19 A. B. Tamayo, S. Garon, T. Sajoto, P. I. Djurovich, I. M. Tsyba, R. Bau and M. E. Thompson, *Inorg. Chem.*, 2005, **44**, 8723.
20 N. Armaroli, G. Accorsi, M. Holler, O. Moudam, J. Nierengarten, Z. Zhou, R. T. Wegh and R. Welter, *Adv. Mater.*, 2006, **18**, 1313.
21 H. J. Bolink, L. Cappelli, E. Coronado, M. Grätzel and M. Nazeeruddin, *J. Am. Chem. Soc.*, 2006, **128**, 46.
22 H. J. Bolink, L. Cappelli, E. Coronado, M. Grätzel, E. Ortí, R. D. Costa, P. M. Viruela and M. Nazeeruddin, *J. Am. Chem. Soc.*, 2006, **128**, 14786.
23 Q. Zhang, Q. Zhou, Y. Cheng, L. Wang, D. Ma, X. Jing and F. Wang, *Adv. Funct. Mater.*, 2006, **16**, 1203.
24 M. K. Nazeeruddin, R. T. Wegh, Z. Zhou, C. Klein, Q. Wang, F. De Angelis, S. Fantacci and M. Grätzel, *Inorg. Chem.*, 2006, **45**, 9245.
25 H. J. Bolink, L. Cappelli, E. Coronado, A. Parham and P. Stössel, *Chem. Mater.*, 2006, **18**, 2778.
26 H.-C. Su, F.-C. Fang, T.-Y. Hwu, H.-H. Hsieh, H.-F. Chen, G.-H. Lee, S.-M. Peng, K.-T. Wong and C.-C. Wu, *Adv. Funct. Mater.*, 2007, **17**, 1019.
27 H.-C. Su, C.-C. Wu, F.-C. Fang and K.-T. Wong, *Appl. Phys. Lett.*, 2006, **89**, 261118.
28 J. D. Slinker, J. Rivnay, J. S. Moskowitz, J. B. Parker, S. Bernhard, H. D. Abruña and G. G. Malliaras, *J. Mater. Chem.*, 2007, **17**, 2976.
29 L. He, L. Duan, J. Qiao, R. Wang, P. Wei, L. D. Wang and Y. Qiu, *Adv. Funct. Mater.*, 2008, **18**, 2123.
30 E. Z. Colman, J. D. Slinker, J. B. Parker, G. G. Malliaras and S. Bernhard, *Chem. Mater.*, 2008, **20**, 388.
31 H.-C. Su, H.-F. Chen, F.-C. Fang, C.-C. Liu, C.-C. Wu, K.-T. Wong, Y.-H. Liu and S.-M. Peng, *J. Am. Chem. Soc.*, 2008, **130**, 3413.
32 S. Graber, K. Doyle, M. Neuburger, C. E. Housecroft, E. C. Constable, R. D. Costa, E. Ortí, D. Repetto and H. J. Bolink, *J. Am. Chem. Soc.*, 2008, **130**, 14944.
33 H. J. Bolink, E. Coronado, R. D. Costa, E. Ortí, M. Sessolo, S. Graber, K. Doyle, M. Neuburger, C. E. Housecroft and E. C. Constable, *Adv. Mater.*, 2008, **20**, 3910.
34 H. J. Bolink, E. Coronado, R. D. Costa, N. Lardiés and E. Ortí, *Inorg. Chem.*, 2008, **47**, 9149.
35 H.-C. Su, H.-F. Chen, C.-C. Wu and K.-T. Wong, *Chem.–Asian J.*, 2008, **3**, 1922.
36 X. Zeng, M. Tavasli, I. F. Perepichka, A. S. Batsanov, M. R. Bryce, C.-J. Chiang, C. Rothe and A. P. Monkman, *Chem.–Eur. J.*, 2008, **14**, 933.
37 T.-H. Kwon, Y. H. Oh, I.-S. Shin and J.-I. Hong, *Adv. Funct. Mater.*, 2009, **19**, 711.
38 L. He, J. Qiao, L. Duan, G. F. Dong, D. Q. Zhang, L. D. Wang and Y. Qiu, *Adv. Funct. Mater.*, 2009, **19**, 2950.
39 C. Rothe, C.-J. Chiang, V. Jankus, K. Abdullah, X. Zeng, R. Jitchati, A. S. Batsanov, M. R. Bryce and A. P. Monkman, *Adv. Funct. Mater.*, 2009, **19**, 2038.
40 R. D. Costa, Enrique Ortí, H. J. Bolink, S. Graber, S. Schaffner, M. Neuburger, C. E. Housecroft and E. C. Constable, *Adv. Funct. Mater.*, 2009, **19**, 3456.
41 R. D. Costa, E. Ortí, H. J. Bolink, S. Graber, C. E. Housecroft, M. Neuburger, S. Schaffnerb and E. C. Constable, *Chem. Commun.*, 2009, 2029.
42 R. D. Costa, F. J. Céspedes-Guirao, E. Ortí, H. J. Bolink, J. Gierschner, F. Fernández-Lázaro and A. Sastre-Santos, *Chem. Commun.*, 2009, 3886.
43 L. He, L. Duan, J. Qiao, G. Dong, L. Wang and Y. Qiu, *Chem. Mater.*, 2010, **22**, 3535.
44 R. D. Costa, E. Ortí, H. J. Bolink, S. Graber, C. E. Housecroft and E. C. Constable, *J. Am. Chem. Soc.*, 2010, **132**, 5978.
45 R. D. Costa, E. Ortí, H. J. Bolink, S. Graber, C. E. Housecroft and E. C. Constable, *Adv. Funct. Mater.*, 2010, **20**, 1511.
46 M. Mydlak, C. Bizzarri, D. Hartmann, W. Sarfert, G. Schmid and L. De Cola, *Adv. Funct. Mater.*, 2010, **20**, 1812.
47 H.-C. Su, Y.-H. Lin, C.-H. Chang, H.-W. Lin, C.-C. Wu, F.-C. Fang, H.-F. Chen and K.-T. Wong, *J. Mater. Chem.*, 2010, **20**, 5521.
48 C.-H. Yang, J. Beltran, V. Lemaur, J. Cornil, D. Hartmann, W. Sarfert, R. Fröhlich, C. Bizzarri and L. De Cola, *Inorg. Chem.*, 2010, **49**, 9891.
49 H.-F. Chen, K.-T. Wong, Y.-H. Liu, Y. Wang, Y.-M. Cheng, M.-W. Chung, P.-T. Chou and H.-C. Su, *J. Mater. Chem.*, 2011, **21**, 768.
50 H.-C. Su, H.-F. Chen, Y.-C. Shen, C.-T. Liao and K.-T. Wong, *J. Mater. Chem.*, 2011, **21**, 9653.
51 L. He, L. Duan, J. Qiao, D. Zhang, L. Wang and Y. Qiu, *Chem. Commun.*, 2011, **47**, 6467.
52 M. Lenes, G. Garcia-Belmonte, D. Tordera, A. Pertegás, J. Bisquert and H. J. Bolink, *Adv. Funct. Mater.*, 2011, **21**, 1581.
53 C.-C. Ho, H.-F. Chen, Y.-C. Ho, C.-T. Liao, H.-C. Su and K.-T. Wong, *Phys. Chem. Chem. Phys.*, 2011, **13**, 17729.
54 C.-T. Liao, H.-F. Chen, H.-C. Su and K.-T. Wong, *J. Mater. Chem.*, 2011, **21**, 17855.
55 C.-T. Liao, H.-F. Chen, H.-C. Su and K.-T. Wong, *Phys. Chem. Chem. Phys.*, 2012, **14**, 1262.
56 H.-B. Wu, H.-F. Chen, C.-T. Liao, H.-C. Su and K.-T. Wong, *Org. Electron.*, 2012, **13**, 483.
57 Y. Zheng, A. S. Batsanov, R. M. Edkins, A. Beeby and M. R. Bryce, *Inorg. Chem.*, 2012, **51**, 290.
58 V. Sivasubramaniam, F. Brodkorb, S. Hanning, H. P. Loebl, V. V. Elsbergen, H. Boerner, U. Scherf and M. Kreyenschmidt, *Cent. Eur. J. Chem.*, 2009, **7**, 836.
59 K. W. Lee, J. D. Slinker, A. A. Gorodetsky, S. Flores-Torres, H. D. Abruña, P. L. Houston and G. G. Malliaras, *Phys. Chem. Chem. Phys.*, 2003, **5**, 2706.
60 C.-Y. Liu and A. J. Bard, *Appl. Phys. Lett.*, 2005, **87**, 061110.
61 D. Hohertz and J. Gao, *Adv. Mater.*, 2008, **20**, 3298.

62 R. J. Holmes, S. R. Forrest, T. Sajoto, A. Tamayo, P. I. Djurovich, M. E. Thompson, J. Brooks, Y.-J. Tung, B. W. D'Andrade, M. S. Weaver, R. C. Kwong and J. J. Brown, *Appl. Phys. Lett.*, 2005, **87**, 243507.
63 B. Park, Y. H. Huh, H. G. Jeon, C. H. Park, T. K. Kang, B. H. Kim and J. Park, *J. Appl. Phys.*, 2010, **108**, 094506.
64 C. C. Chi, C. L. Chiang, S. W. Liu, H. Yueh, C. T. Chen and C. T. Chen, *J. Mater. Chem.*, 2009, **19**, 5561.
65 S. Wang, J. Zhang, Y. Hou, C. Du and Y. Wu, *J. Mater. Chem.*, 2011, **21**, 7559.
66 Y. Shao, G. C. Bazan and A. J. Heeger, *Adv. Mater.*, 2007, **19**, 365.
67 M. Cocchi, V. Fattori, D. Virgili, C. Sabatini, P. D. Marco, M. Maestri and J. Kalinowski, *Appl. Phys. Lett.*, 2004, **84**, 1052.
68 Y. Sun and S. R. Forrest, *Appl. Phys. Lett.*, 2007, **91**, 263503.
69 N. Chopra, J. Lee, Y. Zheng, S.-H. Eom, J. Xue and F. So, *Appl. Phys. Lett.*, 2008, **93**, 143307.
70 R. Wang, D. Liu, H. Ren, T. Zhang, H. Yin, G. Liu and J. Li, *Adv. Mater.*, 2011, **23**, 2823.

